Morphological characterization of well defined methacrylic based di- and triblock ionomers

L. N. Venkateshwaran*, G. A. York†, C. D. DePorter‡, J. E. McGrath‡, and G. L. Wilkes§**

Departments of ‡Chemistry and §Chemical Engineering and Polymer Materials and Interfaces Laboratory, Virginia Polytechnic Institute and State University, Blacksburg, VA 24061, USA

(Received 8 April 1991; accepted 12 August 1991)

A detailed morphological investigation of methacrylic based block ionomers was conducted. In the case of the triblock systems, the end blocks were based on t-butyl methacrylate while the elastomeric centre block was either n-hexyl methacrylate or 2-ethylhexyl methacrylate. Upon hydrolysis of the end block the acid form of the block polymer was obtained. Neutralization of this component led to the ionic block polymer. The effect of ionic block length and the consideration of either di- or triblock architecture was studied. Though the diblock materials exhibited poor tensile properties relative to the triblock systems, the morphological features of the diblock materials were very interesting when in ionic form. Multiple scattering peaks were observed in the diblock ionomers using SAXS and this was attributed to the well ordered regions that were also observed utilizing TEM measurements. In general, good correspondence between the TEM and SAXS results was obtained. Surprisingly, long range order was less pronounced in the triblock ionomer with similar ion content when compared with its diblock analogue. Finally, the interdomain distance between the ionic domains was found to be highly dependent on ionic block length.

(Keywords: ionomers; morphological characterization)

INTRODUCTION

The introduction of small amounts of ionizable functionalities in polymeric systems considerably changes the mechanical, thermal, morphological and rheological properties. These property variations are due to an aggregation mechanism of the ionic groups to form domains. Of particular interest are those materials termed ionomers which typically contain <15 mol% ionic groups. There have been many theories proposed concerning the features of these aggregations of domains[1–9]. To date, there has been no universal consensus reached regarding the arrangement of the ionic species in these polymers. Most of the earlier studies have focused on ionomers where the charged groups are randomly placed along the polymer chain. Of late, there has been emphasis on studying ionomers containing ionic groups that are located at well defined positions along the polymeric backbone, such as telechelic ionomers[10] and segmented ionomers[11,12].

There has also been an interest in including blocks or sequences of ionic functionalities within the polymeric backbone as a means of possibly promoting new structure–property behaviour[13–15]. These block ionomers are a natural extension of the telechelic or segmented ionomers where instead of one ionic unit at terminal points or per segment, one now has a block which may contain many ionic functionalities in succession. However, only limited information is available in the literature regarding the structure–property behaviour of such block materials[16,17].

McGrath and co-workers[14,18,19] have pioneered the efforts in this field introducing the concept of block ionomers. They have directed their attention toward synthesizing block copolymers where the ionomer block was prepared by the hydrolysis and neutralization of poly(alkyl methacrylates). While some systems have been prepared, these systems have not been characterized in terms of their morphology. Gauthier and Eisenberg[15] have reported the thermal and dynamic mechanical behaviour of styrene-4-vinylpyridinium ABA block ionomers. They observed only one glass transition temperature (T_g) corresponding to the polystyrene phase from thermal analysis. The second T_g (~ 200°C) corresponding to the 4-vinylpyridinium block was not accessible experimentally since the material dequaternized at a lower temperature (~ 150°C). In a recent study, Gouin *et al.*[17] have reported the morphology of an ABA block ionomer using small angle X-ray scattering (SAXS). The ABA block ionomer consists of 4-vinylpyridinium as the short ionic terminal blocks with polystyrene being the non-ionic middle block. A broad asymmetric maximum was observed for all the samples studied. This has been interpreted to arise due to the periodic spacing between the ionic domains. They observed that this periodic spacing was found to be a strong function of the ionic block length.

* Present address: Amoco Chemical Company, Amoco Research Center, PO Box 3011, MS-C1, Naperville, IL 60566, USA
† Present address: Shell Development Co., Westhollow Research Center, PO Box 1380, Houston, TX 77251, USA
** To whom correspondence should be addressed

0032-3861/92/112277-10

It has been shown in the literature[20,21] that sulphonate ionomers associate more strongly than their carboxylate counterparts thereby providing a more stable network structure. The stronger interactions in the sulphonate ionomers have been attributed to the fact that the corresponding acid, namely, sulphonic acid is a much stronger acid than carboxylic acid[22]. One of the limitations of the sulphonic acid based ionomers is if these groups are not quantitatively neutralized, they can undergo thermal degradation at higher temperatures. To overcome this problem, one could use a sequence of carboxylate groups by which the network properties of a sulphonate ionomer might be mimicked. However, a higher ion content would be likely required in the carboxylated block ionomers in order to achieve comparable properties to that of the sulphonate ionomers. If the higher ion content does not pose any potential problems, the carboxylated block ionomers could then possibly provide an equivalent mechanical performance of the sulphonate ionomers yet would not have any of the deleterious effects that were found in the sulphonate ionomers. Of course, it is realized that the greater network stability may possess an inherent limitation—that of increased processing temperatures. It is the objective of this paper to address carboxylated block ionomers and more specifically their structure–property behaviour.

EXPERIMENTAL

Materials

The methacrylate precursors were synthesized by anionic polymerization techniques using the 1:1 adduct of s-butyllithium and 1,1-diphenylethylene as the initiator using the sequential addition technique. The rigid blocks were based on t-butyl methacrylate (TBMA, $T_g \sim 118°C$) while the elastomeric blocks were based on either n-hexyl methacrylate (NHMA, $T_g \sim -10°C$) or 2-ethylhexyl methacrylate (EHMA, $T_g \sim -27°C$). The methacrylate precursors were subsequently hydrolysed using *p*-toluene sulphonic acid to obtain the corresponding acid form, i.e. blocks of polymethacrylic acid. The conditions used give exclusive hydrolysis of the TBMA block and do not affect the elastomeric segment (NHMA or EHMA). The hydrolysed acid blocks were then neutralized using either KOH or CsOH (or Cs_2CO_3) to obtain the final block ionomer. The details regarding the synthesis of the poly(methacrylates), the process of hydrolysis and subsequent neutralization have been reported elsewhere[13,14]. The physical characteristics of the di- and the triblock ionomers are given in *Table 1*. The ion content in these block ionomers was systematically varied by changing the sequence length of the TBMA blocks during the precursor synthesis. The apparent molecular weights and molecular weight distributions (*MWDs*) of the precursors were determined by size exclusion chromatography.

Table 1 Physical characteristics of NHMA/TBMA block ionomers

Sample	Total $\overline{M}_n$	M_w/M_n	NHMA block mol. wt (M_n)	TBMA block mol. wt (M_w)	No. per TBMA block
NT-98/2 (Cs)	52900	1.16	51842	1058	8
NT-96/4 (Cs)	56500	1.21	54240	2260	17
NT-94/6 (Cs)	53600	1.20	50384	3216	25
NT-90/10 (Cs)	55200	1.13	49680	5520	42
TNT-2/96/2 (Cs)	48900	1.26	46944	987	8
TNT-3/94/3 (Cs)	51600	1.28	48504	1548	12
TNT-5/90/5 (Cs)	47100	1.40	42390	2355	18

Nomenclature

The nomenclature used for the samples can be best explained using an example. The designation TNT-5/90/5 (K) refers to a triblock ionomer with NHMA as the elastomeric block, with the composition of the precursor (ester) being 5% TBMA, 90% NHMA and 5% TBMA by weight, neutralized with KOH. Similarly, NT-90/10 (Cs) would correspond to a diblock ionomer with NHMA as the elastomeric segment, with the composition of the precursor being 90% NHMA and 10% TBMA by weight, neutralized with CsOH. In the text, the poly(methacrylic acid) obtained from the hydrolysis of the TBMA segments will be referred to as h-TBMA and the neutralized form as nh-TBMA. The notation N will be replaced by E for the EHMA based materials. All the ionomers were neutralized to the stoichiometric end point, as determined with phenolphthalein indicator.

CHARACTERIZATION

Mechanical properties

The tensile properties were determined using an Instron model 1122. Dog-bone shaped samples measuring 10 mm in length (gauge) and 2.8 mm in width were tested at an initial strain rate of 20 mm min^{-1}.

Small angle X-ray scattering

The SAXS experiments were conducted on an automated Kratky slit collimated camera. The X-ray source was a Phillips generator PW1729. Cu Kα radiation with a wavelength of 1.542 Å was obtained from a Cu target after Ni foil filtering. The scattered intensity was monitored by a one-dimensional position sensitive detector (Innovative Technology Inc.).

Transmission electron microscopy

A Phillips EM-420 scanning transmission electron microscope (STEM) was operated in the transmission mode at 100 kV. Objective and condenser apertures of 30 and 50 μm were used, respectively. Ultrathin sections of the block ionomer samples were microtomed at $\sim -60°C$ using a Reichert-Jung Ultracut with a FC-4 cryo attachment and diamond knife. Hexamethyldisiloxane was used as a liquid substrate to float the microtomed sections.

RESULTS AND DISCUSSION

Effect of ion incorporation

The effect of increasing the block length of the precursor (TBMA–EHMA–TBMA block copolymer) on the observed stress–strain properties is shown in *Figure 1*. As expected, both the modulus and the tensile stress of the material increases with increasing TBMA block length. Since the solubility parameters of TBMA ($\delta = 8.94\ cal^{1/2}\ cm^{-1/2}$) and EHMA ($\delta = 8.46\ cal^{1/2}\ cm^{-1/2}$) are very similar, considerable mixing between the two segments is expected. This being so, the resulting block copolymer would be expected to exhibit a more glassy behaviour at ambient temperature since the T_g would

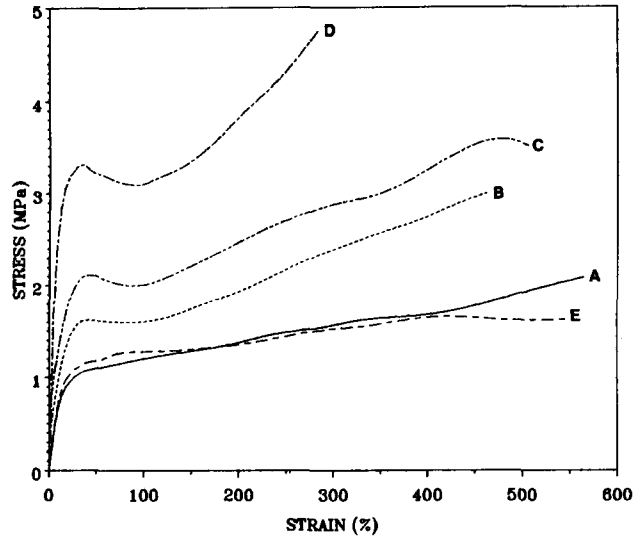

Figure 1 Stress–strain behaviour of the EHMA and EHMA–TBMA copolymers: (A) TET-1/98/1 (K); (B) TET-2/96/2 (K); (C) TET-3/94/3 (K); (D) TET-4/92/4 (K); (E) EHMA

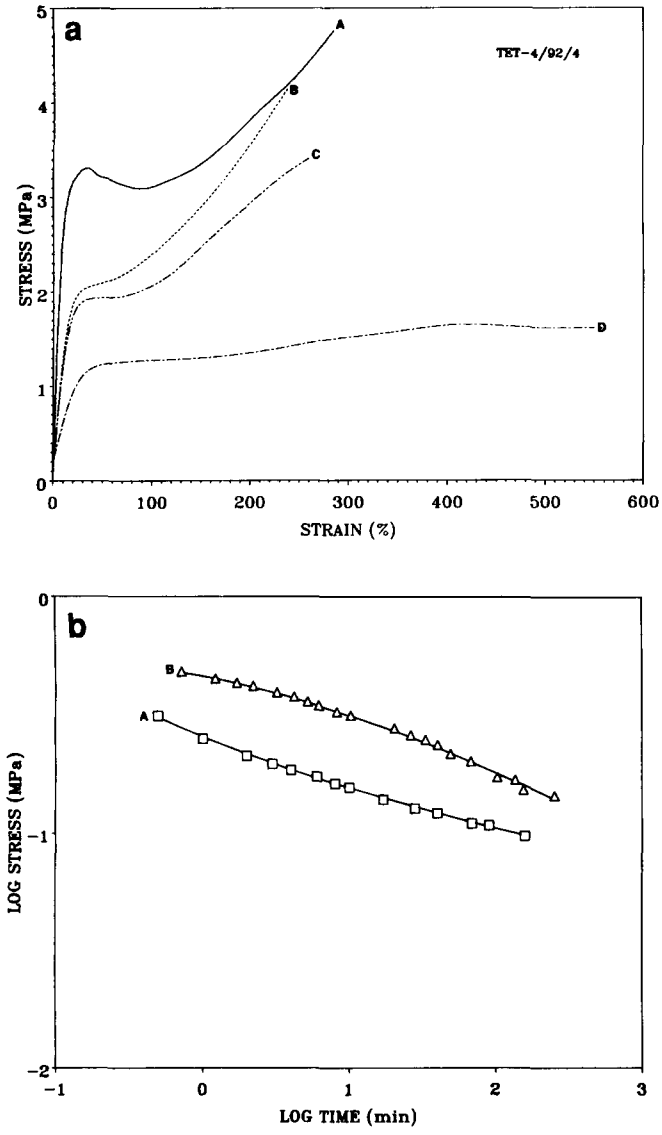

Figure 2 Effect of ion incorporation on the bulk properties of TET ionomers. (a) Stress–strain behaviour: (A) precursor; (B) acid; (C) ionomer; (D) EHMA. (b) Stress–relaxation behaviour: (A) acid; (B) ionomer

now be shifted to a higher temperature. Note that above 2% TBMA content, all the block copolymers exhibit a distinct yielding behaviour. Such behaviour is often observed in glassy or leathery systems when the resistance to deformation is overcome by the applied force.

Changing the polarity of the medium significantly alters the morphological features in the TET materials. *Figures 2a* and *b* show the stress–strain and the stress–relaxation behaviour of the TET 4/92/4(K) block material, respectively. Curve D (EHMA homopolymer) in *Figure 2a* serves as a reference material for comparison purposes. Notice that on incorporation of 8% of the TBMA block with a 92% EHMA backbone (curve A in *Figure 2a*), a substantial *increase* in both the modulus and the tensile stress is observed which is also believed to be due to a high degree of mixing between the TBMA and EHMA segments. On hydrolysis of the TBMA segments, some degree of phase separation takes place due to the much more polar nature of the h-TBMA acid blocks which are formed on hydrolysis. This promotes considerable demixing of the h-TBMA and EHMA segments. The demixing process substantially decreases both the modulus and tensile stress of the material since there will now be two T_gs associated with the system, one for the rubbery backbone matrix and the other for the h-TBMA segments. Since the continuous EHMA phase will now have a lower T_g, the initial response on deformation will be more rubbery in nature. Hence, the observation of lower modulus and tensile stress (curve B in *Figure 2a*). Neutralization of the acid blocks with KOH promotes *further demixing* between the nh-TBMA and the EHMA segments, resulting in additional lowering of both the modulus and the tensile stress of the material (curve C in *Figure 2a*). The phase separated nh-TBMA segments are believed to form more cohesive domains due to the stronger associations between the ionic groups within the domains, resulting in a greater network stability. However, it was disappointing that the tensile strength was not enhanced and, in fact, displayed somewhat lower values.

Figure 2b shows the stress–relaxation behaviour of the acid and the ionomer of the TET-4/92/4 material. It is noted that the ionomer (curve B in *Figure 2b*) clearly maintains a higher stress over a longer period ($\sim$ 100 min) than the acid (curve A in *Figure 2b*). Recall that from the stress–strain measurements, both the precursor and the acid exhibited a higher modulus and tensile stress (at a given elongation) than the ionomers. As explained earlier, the higher stress is due to the occurrence of phase mixing between the TBMA and EHMA segments. These specific associations are temporal in nature *unlike* the associations within the ionic domains which are stronger. Therefore, more of the initial stress is quickly relaxed during the stress–relaxation experiment for the acid form. The greater network stability or greater stress level in the ionomer is primarily due to its more electrostatic nature which is responsible for the cohesive network formed as a result of the stronger mutual associations within the ionic domains.

SAXS analysis

The SAXS profiles of the precursor, acid and the ionomer for the TET-4/92/4 material are given in *Figure 3a*. No scattering peak was observed for the precursor material which implies a lack of periodicity in the system.

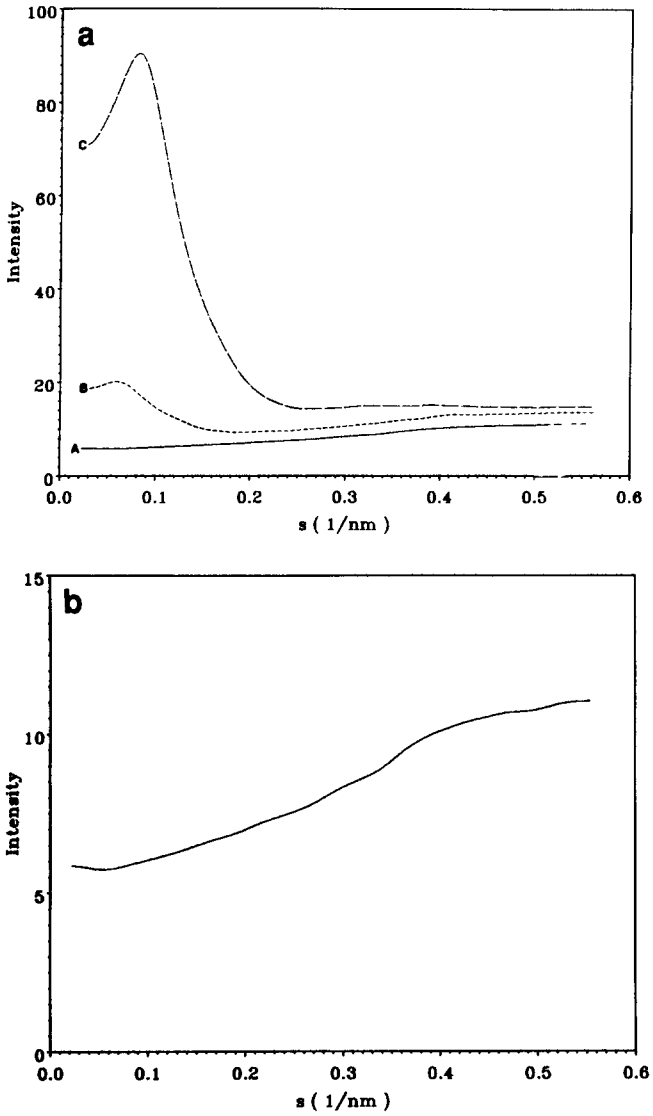

Figure 3 SAXS profiles of the TET-4/92/4 material. (a) Composite plot: (A) precursor, (B) acid; (C) ionomer (w/K). (b) Precursor (ester form). note the expanded scale relative to (a)

However, the lack of observation of the scattering peak may be due to both the TBMA and EHMA segments being phase mixed or that the electron density difference between the two segments is too small to promote a contrast factor to allow an interdomain spacing to be detected. However, the stress–strain measurements seem to imply that the TBMA and EHMA segments are well mixed. Also, from d.s.c. measurements, only a single broad T_g was observed which again indicates that the two segments are phase mixed[23]. On hydrolysis of the TBMA segments, however, a distinct SAXS peak is observed for the acid form. Considerable reorganization due to the association of the polar acid groups must therefore take place. The spacing obtained from the position of the smeared scattering peak is ~14.8 nm. As mentioned earlier, the reorganization of the segments is essentially promoted by the demixing process which arises due to segment incompatibility between the more polar h-TBMA segments and the non-polar EHMA block segments.

On neutralization of the acid groups, there is a *significant* increase in the scattering intensity and the SAXS peak shifts to a somewhat larger value of s or lower estimated spacing (11.9 nm). The increase in the scattering intensity can be attributed to the enhancement of the scattering contrast with neutralization. In addition, the polarity of the nh-TBMA segments increases substantially due to the neutralization procedure which provides a greater driving force for demixing (or phase separation) between the nh-TBMA and the EHMA segments. It is therefore speculated that most of the nh-TBMA segments phase separate from the EHMA matrix resulting in a further lowering of the T_g of the EHMA backbone. The small but distinct shift of the scattering peak to a higher s value (smaller interdomain spacing) may possibly be accounted for by a redistribution in packing density as the phase separation is further promoted by the neutralization. It can be seen from *Figure 3b*, that the high angle region of the precursor exhibits an unusual increase (almost step-like) in the scattered intensity which the authors believe may be due to contributions other than the onset of wide angle X-ray scattering. Background subtraction using some of the common methods discussed in the literature[24,25] resulted in negative intensity values being obtained near s values ~0.2–0.25 nm^{-1}. The origin of the excess scattering at the high angle region is not known at this time but may be a characteristic feature of the precursor. Hence, no further quantitative analysis such as an invariant or the diffuse boundary analysis could be performed for the TET block ionomers with confidence.

Effect of ionic segment architecture

In ionomers, the architectural factors greatly influence the nature of ion aggregation in the system. As shown in the literature, multiplet or cluster formation has been observed in a number of systems in random ionomers where the ion groups are randomly placed along the polymeric backbone[1–9]. In the telechelic systems, however, where the ionic groups are placed only at the chain ends, the multiplets aggregate in an ordered fashion to form supermultiplets and therefore the formation of clusters is unlikely[26]. Hence, the morphology of the ionomers is significantly affected depending on the architectural features of the ionomers. To determine the nature of ion aggregation in these block ionomers, two variations in the architecture have been considered in this study—di- and triblock ionomers. In these systems, the ionic segment was again based on poly(alkali metal methacrylate) derived from poly(t-butyl methacrylate) and the elastomeric or non-ionic segment was based on poly(n-hexyl methacrylate) (NHMA, $T_g = -10°C$).

Stress–strain behaviour

The stress–strain behaviour of the *diblock* ionomers neutralized with K and Cs are shown in *Figures 4a* and *b*, respectively. As expected, these materials essentially flow at ambient conditions and on physical examination, are tacky in nature. This is not surprising since these diblock ionomers can only form a micellar type of structure with the ionic aggregates located in a core surrounded by the elastomeric NHMA chains. The ionic domains which are glassy at room temperature act as a reinforcing filler and provide some resistance to the applied stress which is observed in the stress–strain behaviour up to ~400% elongation. With only one end of the chains anchored, the applied stresses are quickly relaxed by the NHMA segments. In both the K and Cs diblock ionomers, the modulus and the tensile stress at a given strain increases

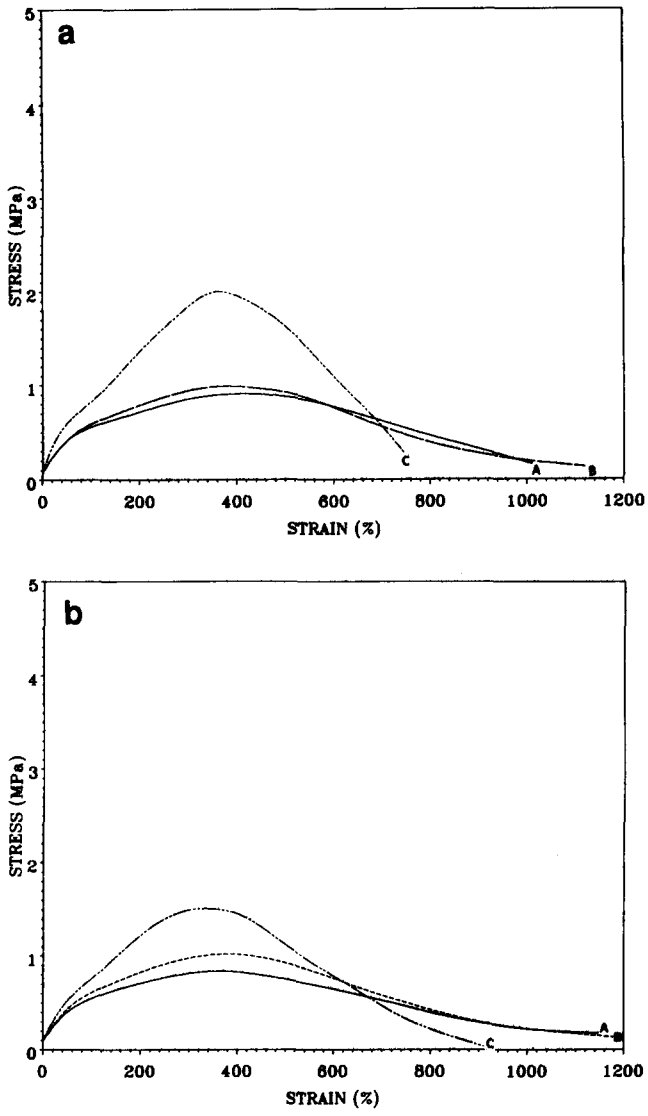

Figure 4 Stress–strain behaviour of NHMA–TBMA diblock ionomers. (a) K ionomers: (A) TN-K-4; (B) TN-K-6; (C) TN-K-10. (b) Cs ionomers: (A) TN-Cs-4; (B) TN-Cs-6; (C) TN-Cs-10

with increasing nh-TBMA block length. With increasing nh-TBMA block length, the ion content in the material increases, resulting in either larger ionic domains and/or an increase in the number of ionic domains in the material, both of which can be responsible for the observed stress–strain behaviour. It is observed that the K ionomers display both a higher modulus and a higher tensile stress than the corresponding Cs ionomer. Since the ionic radius of K (1.33 Å) is smaller than that of Cs (1.69 Å), it is known from electrostatics that the smaller ionic radius results in higher attractive forces within the ionic domains often resulting in a stiffer material and may help explain the observed difference in tensile behaviour of the two ionomers.

A significant improvement in the mechanical properties is expected in going from a diblock to a triblock ionomer. The stress–strain behaviour of the K and Cs triblock ionomers is shown in *Figures 5a* and *b*, respectively. The tensile stress is considerably improved reaching up to ~4–4.5 MPa for material with 10% ion content. Since both ends of the chain can now be potentially anchored in the ionic domains, a higher tensile stress is therefore anticipated. However, these triblock carboxylated ionomers displayed rather poor stress–strain behaviour when compared to linear sulphonated telechelic polyisobutylene ionomers studied earlier in this laboratory[27]. Again, as in the diblock ionomers, both the modulus as well as the tensile stress of the triblock ionomers increases with increasing nh-TBMA block length. The reason for this observed behaviour is exactly the same as that for the diblock ionomers. Also, as in the diblock ionomers, the K ionomers exhibit a higher modulus and tensile strength than the Cs ionomers.

SAXS analysis of the diblock ionomers

The slit smeared and the desmeared SAXS profiles of K and Cs neutralized diblock ionomers are shown in *Figures 6a* and *b* and *7a* and *b*, respectively. Except for the NT-98/2 ionomer, all other ionomers exhibit at least one very distinct SAXS peak and strong evidence of a secondary peak [and even a faint third peak for the NT-90/10 (Cs) ionomer]. The higher angle shoulder is further sharpened on desmearing the slit-smeared SAXS profiles. The scattering peaks represent the periodic spacings between the regions of similar electron density in the material; i.e. the nh-TBMA ionic domains. *Tables 2* and *3* give the periodic spacings between the ionic

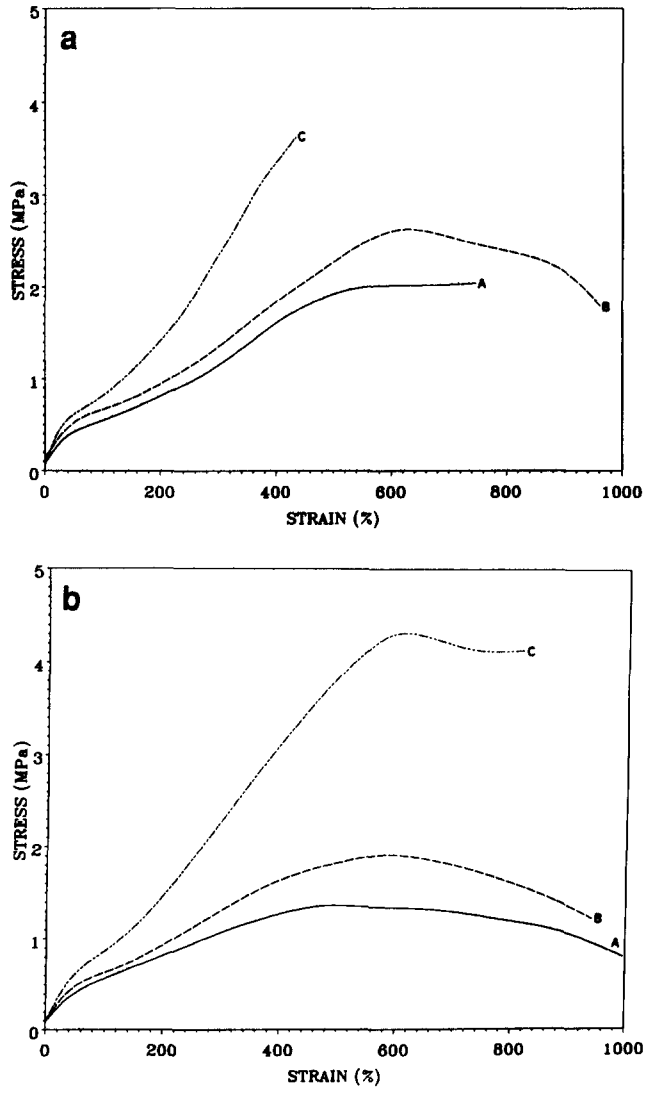

Figure 5 Stress–strain behaviour of neutralized TBMA–NHMA–TBMA (TNT) triblock ionomers. (a) K ionomers: (A) TNT-K-2; (B) TNT-K-3; (C) TNT-K-5. (b) Cs ionomers: (A) TNT-Cs-2; (B) TNT-Cs-3; (C) TNT-Cs-5

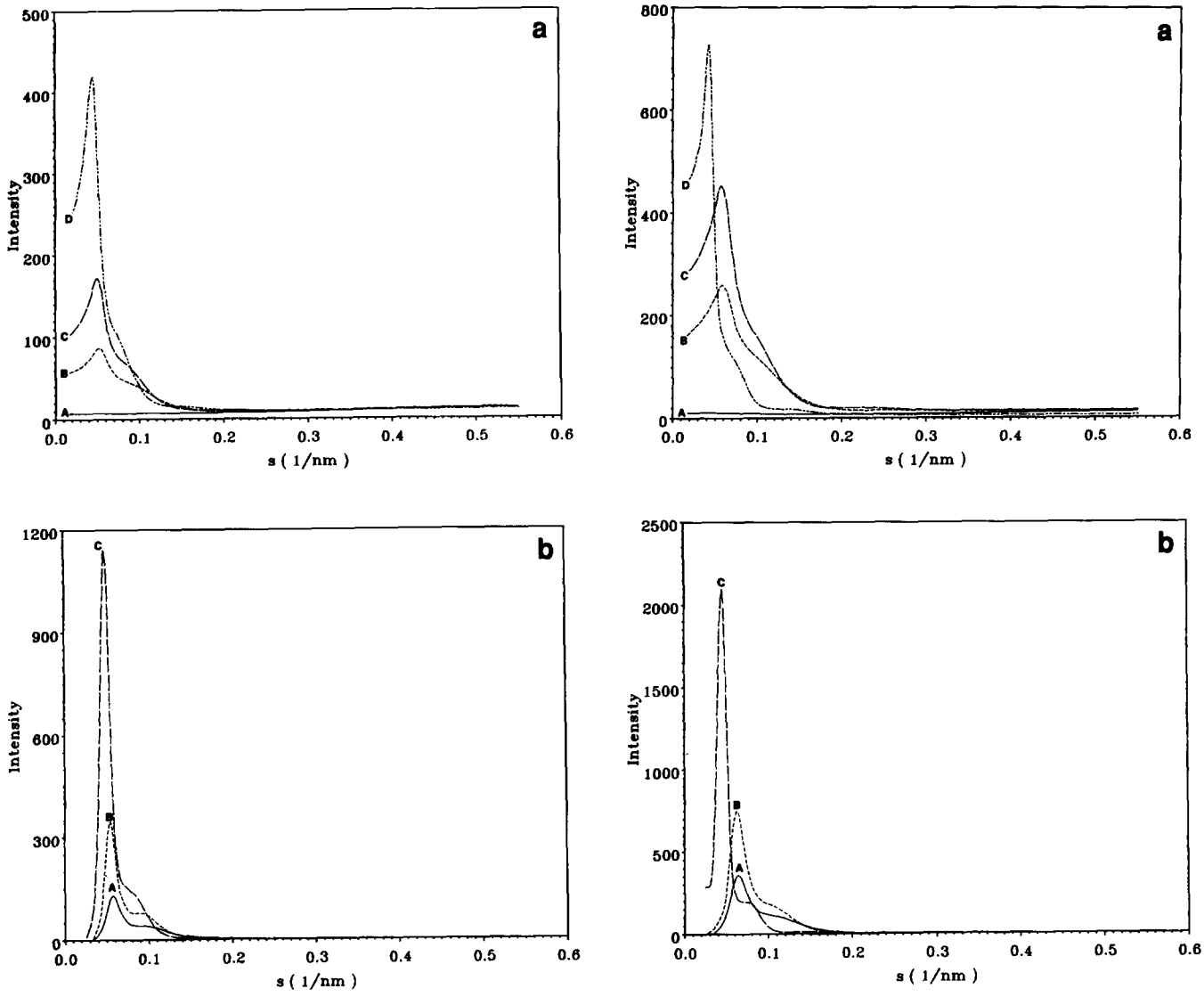

Figure 6 Small angle X-ray scattering profiles of NHMA–TBMA (NT) diblock ionomers neutralized with K. (a) Smeared. (A) NT-98/2; (B) NT-96/4; (C) NT-94/6; (D) NT-90/10. (b) Desmeared: (A) NT-96/4; (B) NT-94/6; (C) NT-90/10

Figure 7 Small angle X-ray scattering profiles of NHMA–TBMA (NT) diblock ionomers neutralized with Cs. (a) Smeared: (A) NT-98/2; (B) NT-96/4; (C) NT-94/6; (D) NT-90/10. (b) Desmeared: (A) NT-96/4; (B) NT-94/6; (C) NT-90/10

Table 2 Periodic spacing between the ionic domains in NHMA–TBMA diblock ionomers as determined by SAXS and TEM analyses

	Periodic spacing between the ionic domains (nm)							
	$d_{smeared}$		$d_{desmeared}$					
Sample	I[a]	II[b]	I	II	$\gamma_1(D)$	$\gamma_3(D)$	TEM	R.m.s.[c]
TN-98/2 (K)								
TN-96/4 (K)	18.8	10.8	17.4	10.0	17.4	20.8		12.9
TN-94/6 (K)	19.8	11.6	18.3	10.6	18.2	22.1		12.5
TN-90/10 (K)	22.3	13.2	21.0	11.8	20.4	24.8	12.5–17.3	12.4
TN-98/2 (Cs)								
TN-96/4 (Cs)	17.0	8.7	15.5	8.6	14.1	18.4		12.9
TN-94/6 (Cs)	17.4	9.9	15.9	9.2	15.4	18.8	13.0–17.3	12.5
TN-90/10 (Cs)	23.8	12.8	23.0	12.7	22.1	26.7	13.5–18.9	12.4

[a] I, Spacing corresponding to the position of the primary SAXS peak
[b] II, Spacing corresponding to the position of the secondary SAXS peak
[c] R.m.s. Unperturbed root mean square end-to-end distance of the NHMA block $=\langle R^2\rangle^{1/2}=(C_\infty nl^2)^{1/2}$ where C_∞ = characteristic ratio, n = number of backbone chain links (or bonds) and l = length of the links (or bonds)

Table 3 Periodic spacing between the ionic domains in TBMA–NHMA–TBMA triblock ionomers and determined by SAXS and TEM analyses

Sample	Periodic spacing between the ionic domains (nm)					
	$d_{smeared}$	$d_{desmeared}$	$\gamma_1(D)$	$\gamma_3(D)$	TEM	R.m.s.
TNT-2/96/2 (K)	13.0	11.9	10.0	13.9		13.0
TNT-3/94/3 (K)	13.5	12.2	10.5	13.9		12.3
TNT-5/90/5 (K)	20.4	18.3	17.1	21.4		11.5
TNT-2/96/2 (Cs)	14.3	13.2	12.8	15.1		13.0
TNT-3/94/3 (Cs)	14.5	13.5	12.9	15.8		12.3
TNT-5/90/5 (Cs)	19.8	18.3	17.0	21.2	18.3	11.5

domains (nh-TBMA) obtained from SAXS and TEM analyses for di- and triblock ionomers, respectively. (Details relating to the TEM analysis will be addressed later.) The SAXS desmeared spacings were obtained using Vonk's desmearing procedure and the periodicities were estimated from analysis of both the one-dimensional (1-D) and the three-dimensional (3-D) correlation functions, respectively, denoted as $\gamma_1(D)$ and $\gamma_3(D)$. The root mean square (r.m.s.) end-to-end distance values for the NHMA block which have been estimated from Gaussian statistics for the unperturbed chains are also provided. The unperturbed r.m.s. end-to-end distance values were calculated from prior knowledge of the characteristic ratio of the NHMA segments using the well known relationship $\langle R^2\rangle^{1/2} = (C_\infty nl^2)^{1/2}$ where C_∞ is the characteristic ratio, n is the number of chain links and 'l' is the length of the connecting units (*Table 2*). The value of C_∞ for NHMA has been reported in the literature[28].

Notice that the positions of both the primary scattering peak as well as the secondary peaks move to lower scattering angles (therefore larger spacings) with increasing block length although the length of the non-ionic block (NHMA) remains nearly the same. There is a very significant increase in the spacing corresponding to the position of the primary peak with increasing ionic block length in comparison to the estimated unperturbed r.m.s. end-to-end distance value of the NHMA chains (*Tables 2* and *3*). Of course, it is realized that the presence of the additional nh-TBMA block would cause an increase in this spacing. However, the increase in the spacing is quite significant, 85% for sample NT-90/10 (Cs) and 59% for sample TNT-5/90/5 (Cs) relative to the estimated r.m.s. values, although the molecular weight of the nh-TBMA blocks is relatively small (*Table 1*). It is, therefore, speculated that the spacing corresponding to the observed scattering peaks is a particularly strong function of the ionic block length. This observation is consistent with the recent work of Gouin *et al.* on styrene-4-vinylpyridium ABA block ionomers[17]. It was also noted in our case that the line widths of the scattering peaks increase with decreasing ionic block length. The larger line width is indicative of a greater dispersity in either the periodic or characteristic spacing between the scattering centres or due to a decrease in the ordering of the macrolattice. As expected, the *intensity* of the scattering peaks increases with increasing ionic block length because of an increase in the volume fraction of the scattering entities (ionic moieties). Based on the spacing obtained from SAXS, it is believed that the ionic blocks are much more extended possibly due to the ionic effects present in the nh-TBMA blocks. In addition, a significant increase in the scattered intensity was observed for the Cs block ionomers as compared to the K block ionomers because of the increase in the scattering contrast promoted by the higher electron density of the Cs species. Recall that sample NT-90/10 (Cs) exhibited a faint third SAXS peak. Since the line width of this peak is very broad, no correlation to any specific morphology could be definitively made.

The periodicity in the electron density fluctuation can also be obtained from the correlation function. The 3-D correlation function, $\gamma_3(D)$, is considered when the assumption of spherical symmetry is valid while the 1-D correlation function, $\gamma_1(D)$, is considered when there is only 1-D symmetry such as may occur in stacked lamellae. More details regarding the utility and interrelation of $\gamma_1(D)$ and $\gamma_3(D)$ can be found elsewhere[29,30]. The 1-D and 3-D correlation functions for the 90/10 diblock ionomers neutralized with K and Cs are shown in *Figures 8a* and *b*, respectively. (Note the considerable oscillation which suggests long range ordering. This oscillation was not a result of Fourier rippling.) In *Table 2*, the spacings obtained from $\gamma_1(D)$ and $\gamma_3(D)$ for the diblock ionomers are provided. These spacings are also indicative of the periodic spacing between the ionic domains assuming 1-D symmetry for $\gamma_1(D)$ and a spherical (or isotropic) symmetry for $\gamma_3(D)$. For the

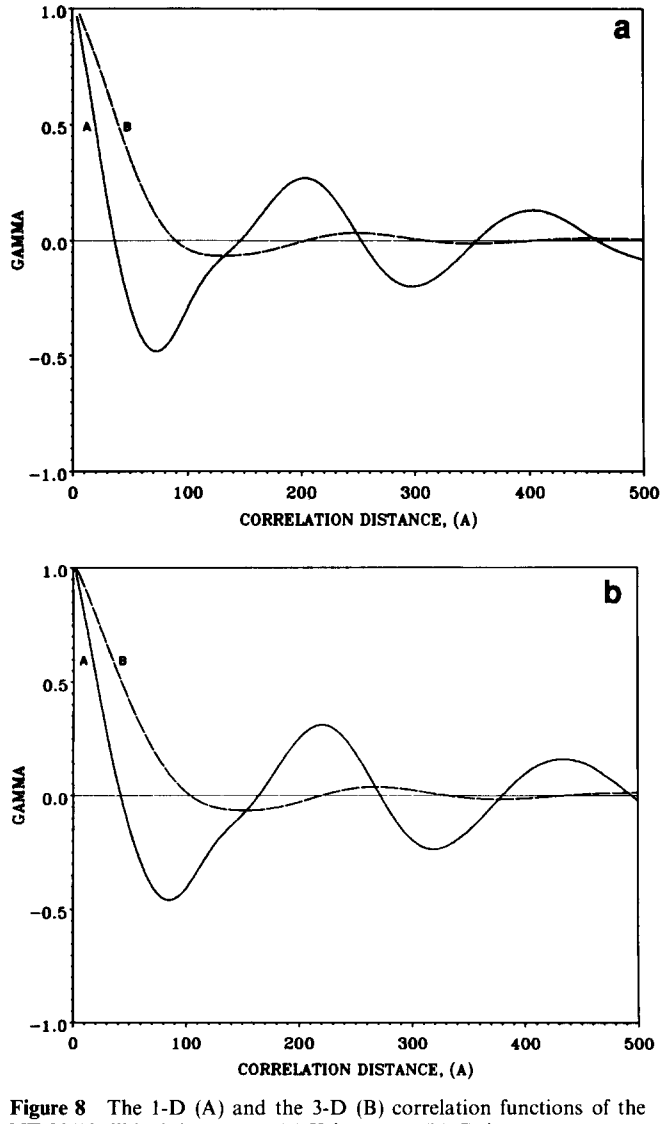

Figure 8 The 1-D (A) and the 3-D (B) correlation functions of the NT-90/10 diblock ionomers: (a) K ionomer; (b) Cs ionomer

diblock ionomers, the desmeared spacings obtained from the SAXS profiles scale more closely to $\gamma_1(D)$ than those from $\gamma_3(D)$. This suggests that the ionic domains might be geometrically anisotropic and may therefore exist in either a stacked cylindrical or a lamellar morphology. Taking the ratio of the primary to the secondary peak provides information regarding the nature of packing of the ionic domains if indeed they pack in a pseudo-lattice. It is well known that for lamellar systems, the ratio of increasing order peaks scale as 1:2:3 while for a hexagonally packed cylindrical system the ratio scales as 1:1.732:2, etc. From *Table 2*, for the diblock ionomers, this ratio ranges between 1.73 and 1.80. Since this ratio is close to 1.732, it is tentatively speculated that the ionic domains may be arranged in a hexagonally packed cylindrical pseudo-lattice. It is also possible that the primary and secondary peaks may be entirely unrelated and that a dual morphology may indeed exist in these systems but this seems doubtful unless some metastable structures are formed due to the preparation conditions or arise from molecular dispersities of the block sizes. However, in order to possibly separate these two hypotheses, imaging the ionic domains using transmission electron microscopy (TEM) was attempted. Sufficient electron density contrast already exists between the block components so that selective staining was not necessary.

TEM analysis of di- and triblock ionomers

The TEM micrographs of the NT-90/10 K and Cs ionomers are shown in *Figures 9a* and *b*, respectively.

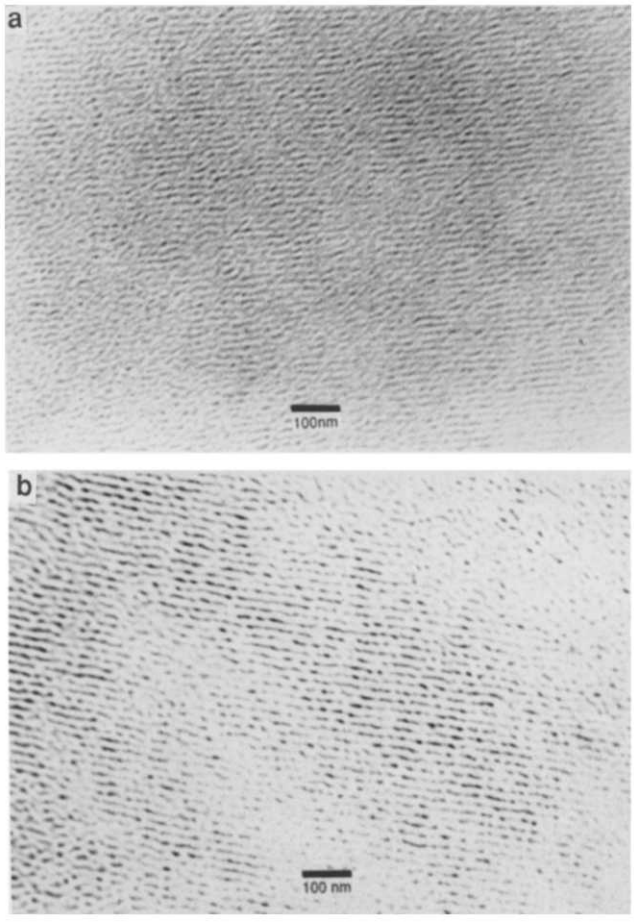

Figure 9 TEM micrographs of NT-90/10 diblock ionomers: (a) K ionomer; (b) Cs ionomer

From the micrographs, both highly ordered as well as somewhat disordered regions can be observed in both the ionomers. A cylindrical or discontinuous lamellar type of structure is observed in the highly ordered regions with an average interdomain spacing of ~19 nm for the NT-90/10 (Cs) ionomer and ~17 nm for the NT-90/10 (K) ionomer—these values being somewhat smaller than the spacing obtained from the position of the primary SAXS peak. However, these are estimated values and do not account for the change in the apparent spacing with possible orientation of the domains with viewing angle in the TEM. Since the ordered regions were randomly arranged with respect to one another, it makes it difficult to determine if these regions were strictly of a lamellar or cylindrical morphological nature. It is anticipated that in view of the ratio of the primary and secondary scattering peaks being 1.73–1.80 and, in view of the relatively low percentage of the ionic block component, the structure is more likely to be of a cylindrical morphology in nature. In addition, such a structure would be well in line with that observed by Feng *et al.*[31] for a ionomer where they found a somewhat cylindrical morphological texture for a system that also possessed a small volume fraction of ionic phase, ~7–10%. It therefore seems that cylindrical texture with the long range order observed in our ionomer block systems is also likely promoted by the strong ionic interactions in these block systems.

It was noted that some disordered regions also existed in the micrographs discussed above. These disordered regions suggested a somewhat spherical morphological texture. This same texture was maintained when the sample was tilted through 45° from the plane of the film in the TEM so as to detect any anisotropy. Since these regions showed a slightly smaller interdomain spacing (13 nm) than the ordered regions, one might attempt to associate this spacing with the secondary peak in the SAXS profile, which is nearly of the same value. However, in view of the fact that the long range order exists in much of the sample, it is believed that the multiple scattering peaks arise from a long range order in contrast to a dual morphology. Moreover, the somewhat disordered regions may also be due to the sample preparation procedure. Future work will attempt to confirm or disprove the proposed speculation.

It is expected that a variation in the ion content would alter the observed morphology. It was observed that decreasing the ion content to 6% in the diblock ionomer by making a shorter ionizable block [sample NT-94/6 (Cs)] shifted the morphology to a more discrete spherical texture (*Figure 10a*). The average spacing for the spherical domains was found to be ~15 nm. Keeping the ion content nearly the same as NT-90/10 (Cs) but changing the architecture to a triblock ionomer [TNT-5/90/5 (Cs), *Figure 10b*], also distinctly shifted the morphology to a disordered spherical structure with the average spacing being ~18 nm. Restated then, with nearly the same ion content, the diblock ionomer exhibits regions of highly ordered morphology but which are surprisingly absent in the corresponding triblock ionomer. The rationale for this observed behaviour will be discussed shortly.

SAXS analysis of the triblock ionomers

For contrast with the SAXS behaviour of the diblock systems, the slit smeared SAXS profiles of K and Cs neutralized triblock ionomers are shown in *Figures 11a*

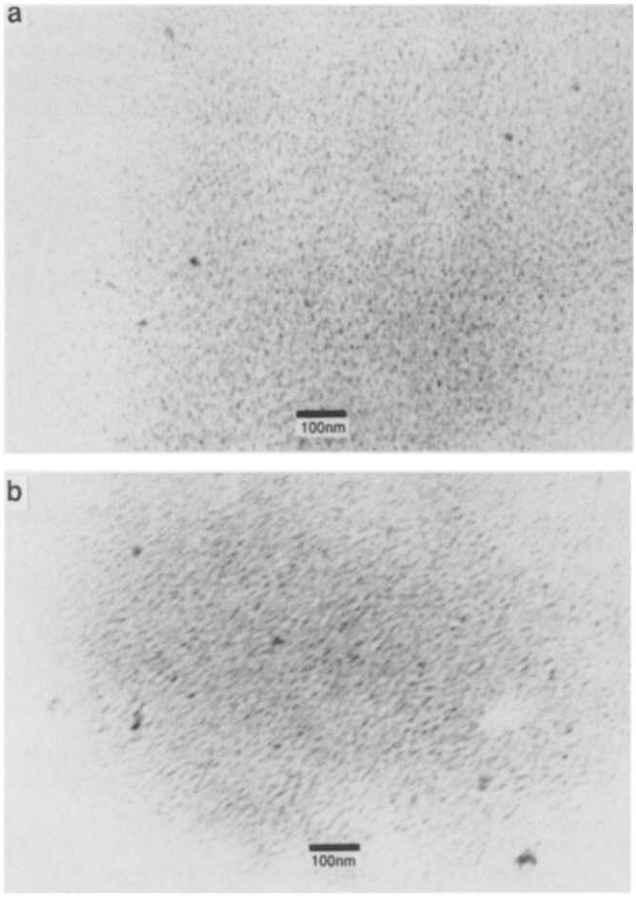

Figure 10 TEM micrographs of Cs neutralized 6% diblock and 10% triblock ionomers: (a) NT-94/6 diblock ionomer; (b) TNT-5/90/5 triblock ionomer

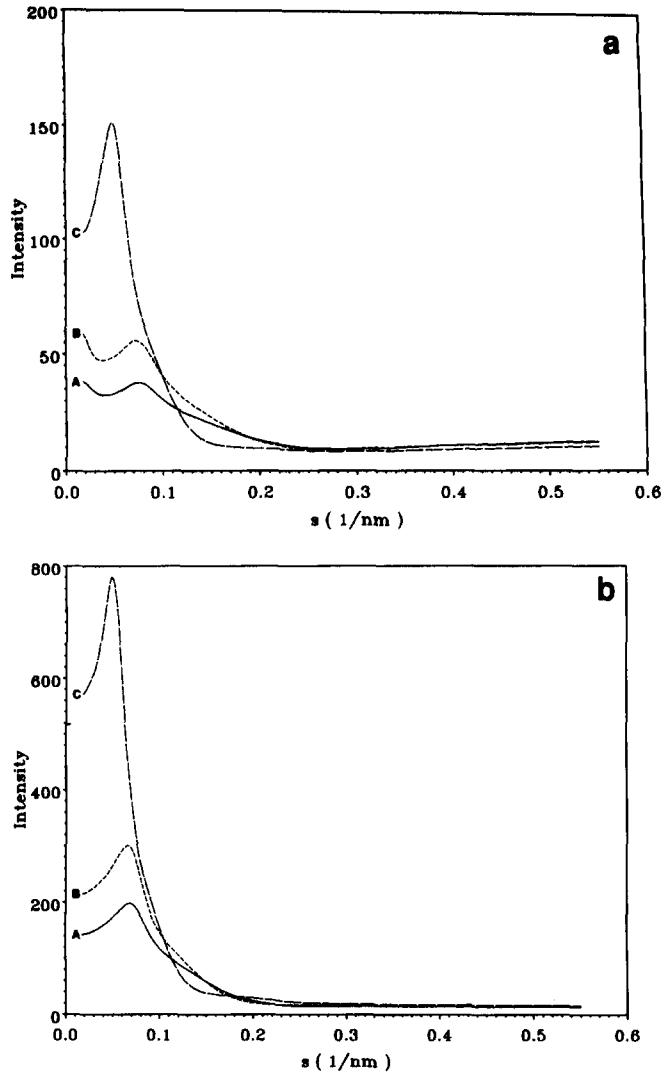

Figure 11 Smeared small angle X-ray scattering profiles of TBMA–NHMA–TBMA triblock ionomers neutralized with (a) potassium and (b) caesium: (A) TNT-2/96/2; (B) TNT-3/94/3; (C) TNT-5/90/5

and *b*, respectively. All the ionomers exhibit a distinct scattering or an ionic peak with the TNT-5/90/5 material of both K and Cs ionomers showing a faint sign of a higher order scattering. *Table 3* provides the periodic spacings between the ionic domains obtained from SAXS and TEM analysis for the triblock ionomers. As mentioned earlier, the SAXS spacings were obtained from the desmearing procedure and also from the analysis of $\gamma_1(D)$ and $\gamma_3(D)$. As in the diblock ionomer, the scattering peak moves to lower scattering angles (therefore larger spacings) and the peak intensity significantly increases with increasing ionic block length. Also, the intensity of the scattering peaks in the Cs ionomers was substantially higher than the K triblock ionomer. These characteristic features in the scattering profile of triblock ionomers are very similar to those observed in the diblock ionomers.

The $\gamma_1(D)$ and $\gamma_3(D)$ values of the K and Cs neutralized TNT-5/90/5 triblock ionomers were also determined as discussed earlier. The periodic spacings obtained from $\gamma_1(D)$ and $\gamma_3(D)$ are also reported in *Table 3*. In the triblock ionomers the desmeared spacings obtained from the SAXS profiles lie between the spacings corresponding to $\gamma_1(D)$ and $\gamma_3(D)$. This again suggests, but does not confirm, that the ionic domains may be geometrically anisotropic in nature. From TEM analysis of the TNT-5/90/5 (Cs) ionomer, mainly spherical domains were observed and there was no indication of any long range ordering. The absence of a distinct secondary scattering peak in the triblock ionomer with the same ion content as that of the diblock ionomer is very surprising. The absence of long range ordering may be tentatively attributed to a larger *MWD* and/or compositional variations of the nh-TBMA segments in the system[32]. Since the compositional distribution of the individual segments is closely related to the *MWD* of the entire polymer, it is often difficult to specifically obtain the compositional distribution of individual segments in block copolymers. However, the apparent *MWD*s of the diblock ionomers are distinctly narrower (1.1–1.2) than those of the triblocks (1.3–1.4) (*Table 1*). The compositional distribution could be attributed to the sequential addition process where the control over the block sequence in the diblock materials is much better than in the triblock materials because of the additional step involved in the synthesis of the precursors for the triblock ionomers. This compositional distribution may potentially be significantly reduced with the use of an active difunctional initiator.

A final point to consider as to why possible differences exist in the morphology of the triblock *versus* the corresponding diblock of equal ionic content is the obvious decrease in the ionic block size by one-half. While we recognize this along with the fact that block length may alter such features as compatibility, we find it difficult to use this aspect to account for the

morphological differences addressed above. Finally, the more discrete domain morphology observed in the diblock ionomers relative to the triblock could also be influenced by the use of the cosolvent methanol (10 vol%) in the case of the triblock ionomers prior to the solution casting step. The cosolvent was not needed for the diblock ionomers—further studies will address this consideration.

SUMMARY

A detailed morphological investigation of methacrylate based block ionomers has been performed. It was found that considerable reorganization within the material takes place with increasing polarity, i.e. from an ester to an acid to an ionomer form of the end blocks. As the polarity of these blocks increases, the demixing of the blocks is greatly facilitated. This is believed to be responsible for the microphase separation of the ionic domains in these block ionomers.

As expected, very poor mechanical properties were observed for the diblock ionomers but the triblock ionomers exhibited some potential for use as pressure sensitive adhesives. Therefore, the potential of using these methacrylate based block ionomers for structural applications, is quite limited although adhesive applications may be of interest.

Multiple scattering peaks were observed from the SAXS experiments for the diblock ionomers which is indicative of a high level of ordering in these systems. This has been confirmed using TEM where highly ordered regions as well as disordered regions were observed. The spacings corresponding to the position of the SAXS peaks appear to correlate very well with the structural features observed from the TEM micrographs. As far as the authors are aware, this is the second study based on an entirely different chemistry where a non-spherical morphology has been observed for a material containing a small volume fraction of the ionic phase. Earlier, Feng *et al.*[31] had observed a non-spherical morphological texture for a segmented ionene system that also possessed a small volume fraction of ionic phase, ~7–10%. Therefore, it seems that the continuous and long range ordered morphology observed here is also likely to be promoted by the strong ionic interactions that take place in these block systems discussed here as well as noted earlier in the segmented ionene systems. Also, the regular placement of ions in both the systems seems to promote the high degree of ordering. At present, no definitive arguments can be made regarding the morphological texture of the ionic domains in these materials, though there is some clear evidence that a cylindrical morphology might indeed be present. Finally, it was found that the periodic spacing between the ionic domains appeared to be a strong function of the ionic block length (nh-TBMA) which has also been suggested in a concurrent study by Gouin *et al.*[17].

ACKNOWLEDGEMENTS

The co-authors (GLW and LNV) gratefully acknowledge the financial support provided by the American Chemical Society—Petroleum Research Fund (no. 19643-AC7-C) for this research. The remaining co-authors also acknowledge the financial assistance of the Dow Chemical Company. A fellowship supplied by the Exxon Chemical company is also gratefully acknowledged.

REFERENCES

1 Eisenberg, A. *Macromolecules* 1970, **3**, 147
2 Eisenberg, A., Hird, B. and Moore, R. B. *Macromolecules* 1990, **23**, 4098
3 MacKnight, W. J., Taggart, T. P. and Stein, R. S. *J. Polym. Sci., Polym. Symp.* 1974, **45**, 113
4 Fujimura, M., Hashimoto, T. and Kawai, H. *Macromolecules* 1982, **15**, 136
5 Yarusso, D. J. and Cooper, S. L. *Macromolecules* 1983, **16**, 1871
6 Yarusso, D. J. and Cooper, S. L. *Polymer* 1985, **26**, 371
7 Lee, D., Register, R. A., Yang, C. and Cooper, S. L. *Macromolecules* 1988, **21**, 998
8 Mauritz, J. *J. Macromol. Sci. Rev. Macromol. Chem. Phys.* 1988, **28**, 65
9 Forman, W. C. *Macromolecules* 1982, **15**, 1032
10 Tant, M. and Wilkes, G. L. *J. Macromol. Sci. Rev. Macromol. Chem. Phys.* 1988, **C28**, 1
11 Feng, D., Venkateshwaran, L. N., Wilkes, G. L., Stark, J. E. and Leir, C. M. *J. Appl. Polym. Sci.* 1989, **37**, 1549
12 Feng, D., Venkateshwaran, L. N., Wilkes, G. L., Leir, C. M. and Stark, J. E. *Am. Chem. Soc., Div. Polym. Chem. Polym. Prepr.* 1988, **29(2)**, 134
13 DePorter, C. D., Venkateshwaran, L. N., York, G. A., Wilkes, G. L. and McGrath, J. E. *Am. Chem. Soc., Div. Polym. Chem. Polym. Prepr.* 1989, **30(1)**, 201
14 Long, T. E., Allen, R. D. and McGrath, J. E. in 'Chemical Reactions on Polymers' (Eds J. L. Benham and J. Kinstle) American Chemical Society, Washington DC, 1988
15 Gauthier, S. and Eisenberg, A. *Macromolecules* 1987, **20**, 760
16 Selb, J. and Gallot, Y. in 'Developments in Block Copolymers—2' (Ed. I. Goodman), Elsevier, London, 1985
17 Gouin, J. P., Williams, C. E. and Eisenberg, A. *Macromolecules* 1989, **22**, 4573
18 Allen, R. D., Huang, T. L., Mohanty, D. K., Huang, S. S., Qin, H. D. and McGrath, J. E. *Am. Chem. Soc., Div. Polym. Chem. Polym. Prepr.* 1983, **24(2)**, 41
19 Allen, R. D., Yilgor, I. and McGrath, J. E. in 'Coulombic Interactions in Macromolecular Systems' (Eds A. Eisenberg and F. E. Bailey) American Chemical Society, Washington DC, 1986
20 Lundberg, R. D. and Makowski, H. S. in 'Ions in Polymers (Ed. A. Eisenberg) American Chemical Society, Washington, DC, 1980, Ch. 2
21 Venkateshwaran, L. N., Tant, M. R., Wilkes, G. L., Charlier, P. and Jerome, R. *J. Appl. Polym. Sci.* in press
22 Lundberg, R. D., Makowski, H. S. and Westerman, M. L. in 'Ions in Polymers' (Ed. A. Eisenberg), American Chemical Society, Washington DC, 1980, Ch. 5
23 DePorter, C. D. unpublished results
24 Koberstein, J. T. and Stein, R. S. *J. Polym. Sci., Polym. Phys. Edn* 1983, **21**, 2181
25 Venkateshwaran, L. N. *PhD Dissertation*, Virginia Polytechnic Institute and State University, 1989
26 Eisenberg, A. and Wollmann, D. *Am. Chem. Soc., Div. Polym. Chem. Polym. Prepr.* 1989, **30(1)**, 201
27 Bagrodia, S., Tant, M. R., Wilkes, G. L. and Kennedy, J. P. *Polymer* 1987, **28**, 2207
28 Mays, J. W. and Hadjichristidis, N. *J. Macromol. Sci. Rev. Macromol. Chem. Phys.* 1988, **C28**, 371
29 Guinier, A. and Fournet, G. 'Small Angle Scattering of X-Rays', J. Wiley & Sons Inc., London, 1955
30 Glatter, O. and Kratky, O. 'Small Angle X-Ray Scattering', Academic Press, New York, 1982
31 Feng, D., Wilkes, G. L., Stark, J. E. and Lier, C. M. *J. Macromol Sci. Chem.* 1989, **A26**, 1151
32 Podesva, J., Stejskal, J. and Kratochvil, P. *Macromolecules* 1987, **20**, 2195